FINAL REPORT

# DESIGN STUDY FOR COUNTERCURRENT DISTRIBUTION (CCD) STUDIES

Contract No. NAS8-32086



February, 1979

Prepared for:

National Aeronautics and Space Administration
George Marshall Space Flight Center
Alabama 35812

BECKMAN®

**Advanced Technology Operations**
Beckman Instruments, Inc.,
1630 South State College,
Anaheim, California 92806

CONTENTS

FIGURES

## SUMMARY

A study was made of various aspects of design of a counter-current distribution (CCD) apparatus for preliminary space flight experiments. A model cell was constructed to ascertain certain performance characteristics. Separation phenomena in the proposed system are observed by optical monitoring. A circulating electrolyte loop acts both to cool the cell and flush away electrolysis products. Cooling may be passive, using only the heat capacity of the rinse medium. Gases are removed by a hydrophilic filter assembly. Reversible electrodes and salt bridge constructions are shown to be infeasible as means for eliminating gas generation and interference by electro-generated ions. The optical system comprises a solid state emitter and compatible phototransistor as detector, both mounted in the body of the cell. A simple amplifier adapts the signal for recording and data interfacing. The entire system is adaptable to relatively compact packaging as a carry-on unit. Automation of the system is feasible, but at high cost, and with a great increase in complexity. It appears possible, depending on the experimental objectives of the principle investigator, to conduct early flight demonstration experiments using a manual system.

## 1.0 INTRODUCTION

The work reported here was conducted under contract NAS-32086, pursuant to contractual change order C04. Its purpose was to support the NASA-sponsored investigation by Dr. Donald E. Brooks, University of British Columbia, on countercurrent distribution (CCD) in space.

In the present context, CCD is the method developed by T. A. Albertsson[1] for separating biological mixtures in two-phase aqueous polymer systems. It is applicable to mixed cell particles as well as macromolecules. A series of chambers is provided, usually in a circular array. Each is filled with the same mixture of two polymers in aqueous solution. The polymers are not fully compatible, so that if shaken and allowed to stand, the mixture separates into

two phases. If a cell particle mixture is added to one of the chambers, then after shaking and standing, particles of any one type tend to partition, in a ratio characteristic of the particle, between the lower phase and the interfacial zone between the phases. This process is extended by multiple transfers, each upper phase (plus the interfacial zone) being shifted onto the lower phase in the next tube, and each shift followed by shaking, settling and again shifting. Different components of the particle mixture thus become differently distributed across the series of tubes. With sufficiently different partition coefficients and a sufficient number of transfers, given components will be isolated in one or several adjacent tubes, completely separated from their neighbors.

A shortcoming of the technique in earth gravity is that large and/or dense cell particles may tend to settle into the lower zone, competing with the normal, selective affinity that might otherwise, for example, bias the partition toward the interface. This can result in a loss of resolution. Implementing the CCD technique in the microgravity of space could therefore significantly enhance the capability of the method. A problem, however, is that gravity is normally relied on for separation of the phases after mixing. An alternative phase separation method must therefore be provided in the space environment. Dr. Brooks[12] has found that this can be accomplished by applying a dc electric field across the mixture, taking advantage of the fact that droplets of either phase, suspended in the other phase, assume a potential with respect to the suspending medium. Phase separation by this process can be rapid enough to make any electrophoretic movement of the sample particles relatively negligible and non-interfering.

The analytical or phase separation space of the CCD cell is typically about 2 or 2.5 mm thick. Its length and width may be about 5 and 0.5 cm, respectively. When adapted for microgravity, it is bounded at its two faces by ion-permeable membranes which may be of microporous, ion-exchange, or other type. Outside of, and adjacent to the membranes, are the electrode-containing chambers. Ports may be provided in these chambers for continuously flushing away gaseous and other electrolysis products. When a dc field is applied, the phases in the middle chamber separate, the interface being about midway in the chamber thickness, and the sample particles are partitioned between the lower phase and the interface as described earlier.

A complete system would have a number of such separation cells, probably disposed a circle, with upper and lower halves of each separation chamber formed as cavities in the mating faces of two flat disks. Initially, with all chambers filled with the phase materials and sample introduced into one of them, the assembly would be shaken, then allowed to equilibrate in the electric field. Rotation of one disk relative to the other would transfer "upper" phase from each chamber onto "lower" phase in the adjacent chamber. Repetition of the shaking, equilibration and transfer would then distribute and separate the sample components around the circular train of cavities.

When Spacelab becomes operational in the near future, it will be feasible to conduct a series of CCD experiments in space that could explore and develop the technique during the course of several flights. Experiments and hardware could progress from a study of basic phenomena to testing of final designs for a multi-stage preparative system.

Beckman Instruments has been called upon to establish general design requirements and operating specifications for an initial flight apparatus. It is expected that many of the design concepts and specifications developed in the study will continue to be applicable to more advanced, fully operative designs.

The proposed first flight unit is a single-chamber device. It is further simplified by omission of any provision for lateral displacement of the phases, one from the other, after equilibration. That is, the phases would not be separately collected at the end of each experiment; rather, the investigation would study phase separation dynamics in situ by probing the cell with an optical beam. Variables in the different experiments could be, for example, the phase composition, various inserted samples, field strength, etc.

## 2.0 OBJECTIVES OF THE STUDY

Beckman undertook to do the following in this study:

### 2.1

Study the possibilities of using reversible, non-gassing electrodes. If feasible, this would simplify the system by eliminating the need for an electrode rinse

arrangement. Relative to this, consider the possible use of salt bridges between the separation chamber and the electrodes to prevent electrolysis products from reaching the separation space. If reversible electrodes and a salt bridge do not appear feasible, define the requirements for an electrode rinse system. Perform bench top experiments as necessary to evaluate design approaches and determine required operating parameter values.

2.2

Define an appropriate system for turbidity measurement. Identify a suitable light source and detector, taking into account the spectral transmission characteristics of typical mixed-phase media. Define an optical geometry compatible with cell design requirements. Specify electronic requirements for source excitation and detector output amplification. Characterize signal level and signal-to-noise ratio.

2.3

Define and test an effective technique for mixing the phases in space. This should be a simple technique compatible with the initial, single-chamber device. Mixing would be done manually, but should be adaptable if necessary to some simple form of automation.

2.4

Develop a conceptual design for an initial CCD flight apparatus embodying features defined and selected in the preceding tasks.

## 3.0 FEASIBILITY OF USING REVERSIBLE ELECTRODES

Reversible electrodes employed in electroanalytical equipment include such types as Ag/AgCl, $Pb/PbSO_4$, and $Cu^0/Cu^{2+}$. Typical electrode reactions are, for example:

$$AgCl + e \rightleftharpoons Ag^0 + Cl^-$$

and

$$Cu^0 - 2e \rightleftharpoons Cu^{++}$$

Another type of reversible electrode to consider is palladium[2,3]. A palladium cathode rapidly absorbs hydrogen generated at its surface, up to an atomic ratio H/Pd of at least 0.5. When such an electrode is reversed, oxygen generated at the surface combines catalytically with the hydrogen dissolved in the metal, so that gaseous oxygen does not appear until the available hydrogen has been largely consumed. A non-gassing electrode pair can therefore comprise an uncharged palladium cathode and a hydrogen pre-charged anode.

Although a number of other types of reversible electrodes are known in the storage battery art, they are not conveniently adaptable to electroanalytical uses. These include the lead-acid, nickel-cadmium and silver-cadmium types, as well as more exotic systems[6] recently developed for high energy density and in some cases for space application.

## 3.1 Required Electrode Characteristics

Reversible electrodes must satisfy several conditions to be useful in the CCD cell:

a. They must accommodate an unusually high current density.

b. They must have a coulombic capacity (charge storage capability) sufficient for at least one typical run.

c. Ions generated at the electrodes (unless isolated from the analysis chamber) must be non-interfering with the analysis.

### 3.1.1 Current Density Considerations

The current density $I_a$ (amperes per $cm^2$ of conducting cross-section) in the CCD cell is

$$I_a = EK_e \qquad (1)$$

where E is the voltage gradient and $K_e$ the electrical conductivity of the medium. Assuming a uniformly conductive medium bridging the path between electrodes, an electrode area equal to the cell cross-section, and electrodes with continuous surfaces (rather than grids), current density at the electrode surface is also given by $I_a$ in (1) above. Our model system assumes $K_e = 5 \times 10^{-2}$ as a maximum and $E = 10$ volt/cm, giving $I_a = 0.5$ amp/$cm^2$.

Current densities at reversible electrodes are limited by the rate at which electrolysis products can diffuse to or from the surface. If one attempts to exceed this limit (by overloading a discharging system or applying excessive voltage on charging), the electrode potential at one or both electrodes becomes sufficient to decompose the water, i.e., to evolve oxygen at the anode and/or hydrogen at the cathode.

Experience shows that a general upper limit to electrode current densities is about 0.05 A/cm$^2$. Lingane[4] cites 0.004 A/cm$^2$ as an upper limit for the Ag/AgCl electrode in 0.1M chloride medium, and 0.05 A/cm$^2$ as general limit in electrodeposition of metals[5]. This same general upper limit of about 0.05 A/cm$^2$ is not even exceeded in heavy duty storage batteries, or recently developed high-energy density batteries[6].

In the palladium electrode discussed earlier, with or without hydrogen presaturation, we are given by Neihof[2] a current density not much above 0.01 A/cm$^2$ before evolution of gas is observed. Reversible electrodes in the CCD therefore appear infeasible on the grounds alone of requiring 10- to 50-fold higher current density than achievable practically. This situation could be eased by expanding the space between the membranes and electrodes in funnel fashion (as a form of salt bridge) to permit electrode areas larger than the cross-section of the separation chamber, but this introduces its own problems (see section 3.4).

### 3.1.2 Required Coulombic Capacity

In view of the preceding, the second and third requirements for reversible electrodes, b) and c) above, are somewhat academic. Nevertheless, it is of interest to consider them briefly.

Assume that it would be convenient to use the reversible electrodes for 10 runs, 4 minutes each, before reversing or recharging them. Taking the current density in our model, as before, at 0.5 A/cm$^2$, each cm$^2$ of electrode surface must support $1.24 \times 10^{-3}$ equivalents of electrochemically active substance. If we take AgCl as an example, considering its density and assuming a packing fraction

(solid volume)/(solid + void) of, say, 0.6, we require the silver surface to be coated with a 0.6 mm thick AgCl layer. This appears feasible, if we compare this value with the thicknesses of coatings that are common, for example, on storage battery plates.

Considering the Pd/H electrode, with its capacity in terms of atomic ratio H/Pd, of up to 0.5, we find that an electrode nominally 0.015" thick provides an electrochemical capacity of $2.5 \times 10^{-3}$ g-equivalents per $cm^2$, more than adequate for our requirements.

Electrochemical capacity as such, then, is not a hindrance to use of reversible electrodes. The problem of ion interference is discussed in the next section.

### 3.1.3 Effect of Electrolysis Products

#### 3.1.3.1 Cations of the Electrode Metal

The metal cations of almost all the reversible electrode systems (e.g., $Ag^+$, $Cu^{2+}$, $Pb^{2+}$) are toxic or inhibitory toward cells and other biological sample materials. Usually, where this has been a problem in electroanalytical systems, the procedure has been to separate the electrodes from the analytical zone by a salt bridge. Thelatter then provides a long enough bridging path that unwanted ions formed at the electrodes do not reach the analytical zone during a run. In CCD, with its typical high current densities and high-conductivity media, salt bridges unfortunately pose a heating problem, as discussed below. Closeness of the electrodes to the sample zone therefore pose a contamination problem.

#### 3.1.3.2 pH Change caused by Electrode Reactions

The Pd/H electrodes, unlike the more familiar reversible types, do not introduce significant amounts of heavy metal cations into the medium. Unfortunately, they do generate a gram-equivalent each of $OH^-$ at the cathode and $H^+$ at the anode per Faraday of charge traversing the cell, again precluding close proximity of the electrodes to the analysis zone. Let us assume that the generated $OH^-$ and $H^+$ each occupy an electrode chamber volume in our model cell of 0.75 ml. Then starting with an unbuffered neutral solution and assuming 1.25 A cell current

and a 4-minute run, the pH on the cathodic and anodic sides should go to 14.6 and -0.6, respectively. Actually, such extremes would not be attained because of the unavailability of sufficient counter-ions to maintain electrical neutrality, given an ostensible generated $OH^-$ and $H^+$ concentration of over 4M. (Expressed differently, polarization prevents maintaining the implied current density.) Further, no buffer composition, even at maximum feasible concentration, could absorb such quantities of generated $H^+$ and $OH^-$ while maintaining pH constant to the desired few hundredths pH unit.

In summary, interference by electrode reaction products, whether by heavy cations, hydrogen ion or hydroxyl ion, is a further bar to the use of reversible electrodes.

## 3.2 Use of Salt Bridges

Salt bridges in electroanalytical equipment usually serve to isolate the electrodes from an analytical zone. They do this by inserting a long electromigration path between these zones. They may also provide dilution and/or buffering to contain the effect of electrolysis products near the electrodes. However, the use of salt bridges in the CCD system is made difficult by heating effects.

The liquid medium of the salt bridge is essentially quiescent, especially in microgravity where thermal convection largely disappears and other circulating forces are small. We avoid mechanical stirring or circulation, if possible, to keep the system simple. Give the usual cell configuration (the analytical chamber thickness being small relative to width and length), it is difficult to interpose a salt bridge long enough and low enough in resistance, between electrodes and analysis space, while maintaining short enough paths for heat flow from the bulk of the salt bridge to a surrounding heat sink.

Schematically (figure 1) the salt bridges would be volumes of quiescent liquid on each side of the analysis chamber. Heat is generated uniformly throughout each volume. The volumes are faced off by parallel heat sink surfaces, for example as at ABFE and DCGH, at constant temperature.

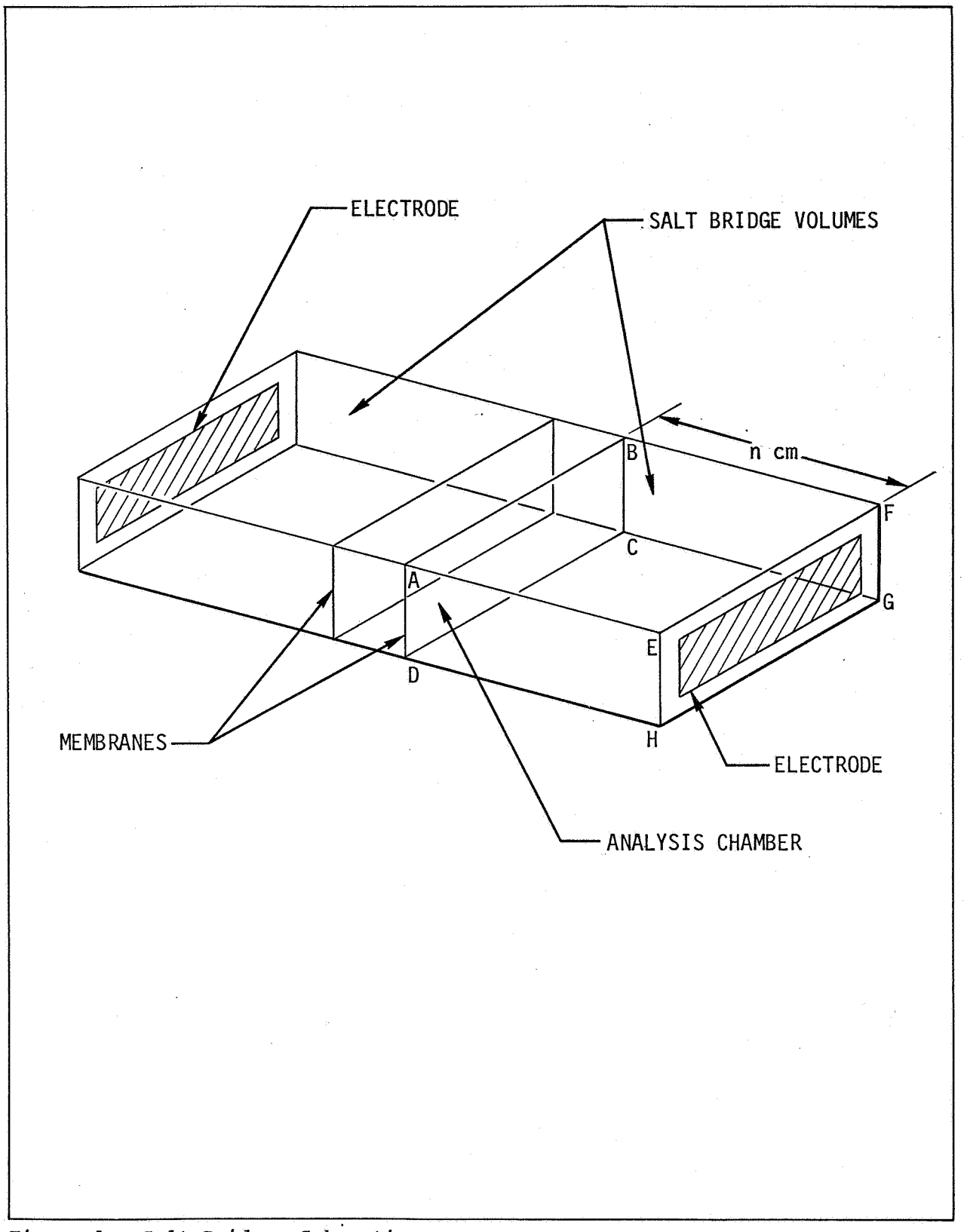


*Figure 1. Salt Bridge, Schematic*

At steady state, temperature elevation, $\Delta T$, in the bridge (measured midway between the heat sinks), relative to the sink temperature, is given approximately by:

$$\Delta T = 0.239\ E^2 K_e d^2 / 2K_t \qquad (2)$$

where $K_e$ is the electrical conductivity of the medium ($ohm^{-1}cm^{-1}$), $K_t$ its thermal conductivity ($cal\ sec^{-1}cm^{-1}deg^{-1}$) and d is the distance between the volume midplane and the heat sinks.

The model analysis chamber is 5 cm long, 0.5 cm wide, 0.25 cm thick. The heat sinks are contiguous with the broad salt bridge faces, 5 cm x 0.5 cm in cross section, and n centimeters long. The value of d is 0.5 cm/2 or 0.25 cm. Taking $K_t = 1.5 \times 10^{-3}$, $K_e = 5 \times 10^{-2}$ and $E = 10$ V/cm, we obtain $\Delta T = 24.9$ degrees. This per se could be tolerable if the heat sink is at, say, 4°C. Consider, however, that the length n of each bridge, even if gel plugs are used to minimize mixing, should be at least about 5 cm. The volume of each bridge is then $(5 \times 0.5 \times 5) = 12.5\ cm^3$. Each $cm^3$ of this volume generates 5 W of power for a total of 62.5 W and a system total of 125 W. This compares with 3.125 W for the analytical zone per se.

Clearly this is an ill-balanced design, and would require a substantial cooling provision, probably of circulating type. Remembering that our interest in salt bridges in the first place was the possible elimination of circulating liquids, the use of cooled salt bridges is not a valid solution.

In summary, analysis indicates that, for various reasons, reversible electrodes are not feasible in a CCD apparatus operating at the required current and wattage densities. The alternative is the use of non-reversible electrodes together with a circulating electrolyte loop that simultaneously cools the analysis chamber and removes electrolysis products from the electrodes.

## 4.0 DESIGN OF THE ELECTRODE RINSE SYSTEM

As shown schematically in figure 2, it is proposed that electrolyte be circulated in a loop which includes the electrode chambers, a liquid/gas phase separator, and a pump. Details relating to filling of the system, start-up, etc., are discussed in a later section.

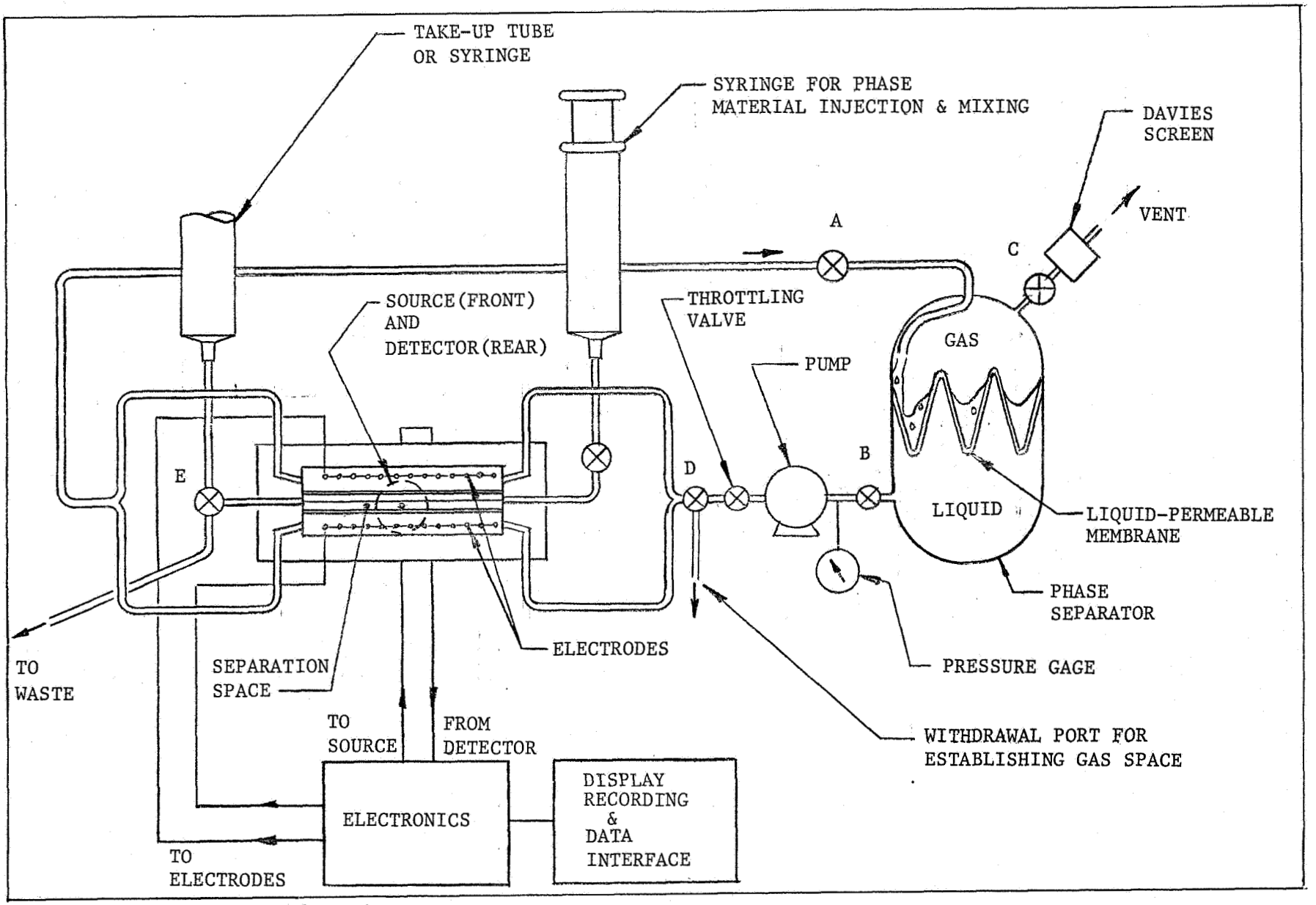


*Figure 2. CCD System, Schematic*

## 4.1 Electrode Chamber Dimensions

The electrode chambers must provide sufficient space between electrodes and membranes so that the gases generated at maximum current can be easily flushed from the cell. Otherwise, large bubbles will obstruct the current and result in a non-uniform, fluctuating field in the sample space. Our experiments show that for typical cell dimensions and a current of 1.5 A (a probable maximum) a flow through each chamber of 5 ml per second will reliably remove the gases. This assumes $O_2$ and $H_2$ generation at theoretical Faradaic equivalence (valid for the $K_2SO_4$ electrolyte used in our experiments.)

For an assumed run of four minutes, the total flow through the electrode chambers is 2.4 liters. This large volume precludes the possibility of "once through" flow of the rinse medium, which if feasible would simplify the system by eliminating the need for a phase separator. Recirculation of the rinse medium therefore appears unavoidable.

## 4.2 Required Rinse Loop Volume

Two considerations affect the required total rinse loop volume: a) the pH change that can be tolerated between replacements of the rinse medium, and b) the required heat capacity, assuming the rinse medium serves as the primary heat sink.

### 4.2.1 pH Stability Requirement

The volume required for pH stability is variable, depending on the electrolyte and the total charge traversing the cell during the experiments. For certain simple electrolytes, e.g., alkali sulfate or phosphate buffer, the net electrode reaction is merely the decomposition of water: if the anodic and cathodic effluents are combined (as we hereafter assume throughout) before being returned to the cell, the solution will remain indefinitely at constant pH. Where the medium contains organic components, however, there may be a gradual, irreversible oxidation at the anode, with possible reduction at the cathode. Depending then on the buffer capacity, if any, of the medium, the pH may drift due to non-equivalence of the hydrogen ion and hydroxyl ions generated.

If the medium is buffered, then addition of small amounts of hydrogen or hydroxyl ion, relative to the amount of buffer present, shifts the pH by approximately

$$\Delta pH = \log_{10} (1 + 2f) \qquad (3)$$

where f is the ratio of added $H^+$ or $OH^-$ to moles of buffer present.

Taking 0.05 pH units as the tolerable pH shift (as suggested by Dr. Brooks), we derive an allowable f value of 0.061. This requirement is easily satisfied with the usual buffer concentrations, as may be shown by the following: assume (worst case) that all the charge transferred during ten 4-minute runs (at 1.25 A) enters into Faraday-equivalent generation of $H^+$ at the anode, with no corresponding cathodic $OH^-$ generation to neutralize the $H^+$ when the effluent streams from the cell are mixed (or the converse: cathodic $OH^-$ generation only, with no anodic $H^+$). The amount of $H^+$ (or $OH^-$) formed is then 0.031 equivalents. If we assume a rinse system volume of 1 liter, then to satisfy the condition $f \lesssim 0.06$, the buffer molarity must be 0.51 or higher. In practice, such disparity of $H^+$ and $OH^-$ generation will almost never occur; and the required buffer molarity will be correspondingly smaller.

### 4.2.2 Cooling Requirement

If the flow rinse system were to be actively cooled, a suitable heat exchanger would be inserted in the rinse loop. We recommend, instead, that the volume of electrolyte in the phase separator (about 1 liter), which serves as mentioned to maintain pH stability, serve also without active cooling as the sink heat. This volume may initially be either at ambient temperature, or may be pre-chilled to about 4°C until the start of the experiment.

Assuming the temperature to be initially at ambient, and (worst case) that all the Joule heat enters the reservoir, we find that temperature elevation in the reservoir even after 10 consecutive runs is quite moderate. The heat generated (g-cal) is given by

$$H = 0.239 K_e E^2 Q t \qquad (4)$$

where E is the voltage gradient (volt/cm), Q the cell volume ($cm^3$) including the spaces between the electrodes and the membranes, and t is the total run time (sec). (The equation neglects Joule heating within the membranes.) Taking $K_e = 5 \times 10^{-2}$, E = 10 volt/cm, Q = 2.13 $cm^3$, and t = 2400 seconds (10 runs, 4 minutes each),

$$H = 6.1 \times 10^3 \text{ g-cal} \qquad (5)$$

or for a one-liter reservoir, a 6.1°C temperature rise. If we assume this to be also the maximum temperature rise at the sink interface (i.e., at the membranes), the maximum temperature rise in the sample space, midway between the membranes, equals this 6.1° plus a calculated 6.2° rise due to heating within the sample chamber itself. Given an ambient temperature of 20°C, the final temperature would be 32°C, a tolerable value for many experiments. In actuality, some of the Joule heat would be lost to the ambient from the connecting tubing, etc., so that our estimate is on the conservative side. With an initial temperature of 4°C in the reservoir, the final temperature would be a modest 16°C (assuming negligible heat leakage from the environment into the reservoir.)

## 4.3 Electrode Chamber Rinse Flow Rate

With an electrode chamber of geometry and dimensions as shown later for the experimental cell, a flow of 5 ml per second in each chamber was found sufficient, with ample margin, to flush electro-generated hydrogen and oxygen reliably from the cell at a current level of 1.5 amps. The electrolyte used was 0.4 M potassium sulfate. The corresponding pressure drop across the cell was 20 inches of water head.

## 4.4 Removal of Electrolytically-Generated Gases

The volume of hydrogen (20°C) generated by the 1.25 amperes during each four-minute run in our model system is 37.4 ml; the corresponding volume of oxygen, 18.7 ml. The practical operation of a circulating system requires that these gases be removed. In an enclosed rinse system, the generated gas presents a problem. Recirculation of the gases through the CCD cell could cause erratic flow, serious fluctuation of the electric field, and pressure build-up.

Electrophoresis systems previously designed for space have used hydrophobic membranes as gas/liquid phase separators. The liquid was retained in the system behind the membranes, and the gases were released. A difficulty experienced with this arrangement was that traces of impurities in the circulation having a surfactant action destroyed the hydrophobicity of the membranes, resulting in escape of electrolyte from the system.

We propose instead a phase separator using an essentially hydrophilic rather than hydrophobic membrane. Integral with the concept is a separator geometry that takes advantage of the unusual behavior of free liquid surfaces in space. With an appropriate geometry, surface tension forces can act to confine and stabilize the liquid phase in a defined zone, while liberating the gaseous phase into a separate, contiguous zone opening to the exterior of the apparatus. It appears that a filter assembly using a fluted filter element can provide the necessary geometry. Related techniques for handling two-phase gas/liquid systems have been the subject of theoretical study[10,11] and application to space-borne systems[7-9]. For example, it is important in fuel tanks used in space that vapor above the fuel not enter into the tank output lines. This was accomplished by fitting the inside of a container with baffles, screens or perforated plates wettable by the liquid.

With gravity essentially eliminated, surface tension effects that are normally significant only in small-diameter or narrow spaces can operate across relatively large dimensions. The dimensions of the system must not be too large, however, otherwise acceleration forces become dominant. The dimensionless Bond member, $B_o$, expresses the relative importance of these contributing factors

$$B_o = F_a/F_c = Ma/\gamma L = \rho L^3 a/\gamma L = \rho L^2 a/\gamma$$

where $F_a$ and $F_c$ are the acceleration and capillary (surface tension) forces, respectively, M is the mass, $\underline{a}$ the acceleration, L the characteristic length, $\gamma$ the surface tension, and $\rho$ the liquid density. When the Bond number is large (greater than 1), acceleration is dominant in shaping the surface; when it is small, surface tension effects dominate.

The shape of the liquid/air interface, with and without gravity, has been derived analytically and by computer for systems of various geometries[11,14]. The form and location of the liquid/air interface at equilibrium satisfy the conditions that:

- The total surface free energy is a minimum;
- The radius of curvature is everywhere constant, or (for surfaces of compound curvature), the value of $(1/r_1 + 1/r_2)$ is everywhere constant, $r_1$ and $r_2$ being the maximum and minimum curvatures at any point.
- The contact angle $\theta$ between the liquid and solid surfaces everywhere satisfies the relation

$$\theta = \arccos \frac{\gamma_{vs} - \gamma_{ls}}{\gamma_{vl}}$$

where $\gamma$ is the interfacial tension and the subscripts vs, ls, and vl refer respectively to the vapor/solid, liquid/solid, and vapor/liquid interfaces.

A consequence of these conditions is that where liquids wet the containing surfaces, they tend to occupy the narrowest accessible spaces. At equilibrium, they expose the minimum area of vapor/liquid interface. By the introduction of baffles, narrow spaces are created where the liquid can be spontaneously localized. To locate the liquid in contact with a fixed position (e.g., an outlet port) independent of the liquid volume during filling or emptying, the containment spaces should taper toward the point of localization[7]. If the baffles are perforated, they are made effectively more wettable, if this should be necessary. The perforations also permit continuous, free redistribution of the liquid to equilibrium positions as the container is filled or emptied.

An experiment closely pertinent to our present program was conducted on board Apollo 14[13]. This used small, shallow assemblies (about 10 cm diameter) which were in effect two-dimensional analogues of liquid storage containers. The transparent faces of the assembly allowed the liquid distribution pattern to be observed and photographed during filling and emptying. The effect of the design is that the liquid body is maintained integral and in contact with the exit port throughout the filling or emptying operation. These same general principles are applied in our proposed use of a fluted, hydrophilic filter as a gas/liquid phase separator. In this arrangement, surface tension forces naturally maintain the liquid within the triangular spaces, where the liquid/gas interfaces will have minimum radii of curvature, and bubbles are forced to the surface.

### 4.4.1 Filter/Phase Separator

Fortunately, commercial filter units are frequently made with a pleated construction which offers just the kind of wedge-shaped spaces that are needed. A view of such a filter element is shown in figure 3A. It is of hollow cylindrical shape, as most such elements are. The element is folded or pleated to increase its surface area and incidentally reduce the pressure drop across the unit. Ordinarily, flow through these units is from the outside to the inside of the annulus. However, for control of the gas-liquid interface in the present application, this will be reversed for the microgravity separator. The mixed-phase input stream will be introduced at the inside of the annulus, and gas-free liquid taken out on the outside. Thus, in the interior of the unit, both the gross geometry as well as the detailed configuration of the pleats is conducive to segregation of the gas from the liquid. The gas accumulates in the center while the liquid equilibrates in the V-shaped spaces on the inside diameter of the filter element. Stability of the interface derives from the fact that the surface free energy is a minimum when the liquid settles uniformly and as deeply as possible within the folds. The liquid surface is everywhere concave toward the gas.

Other important geometric features of the filter separator assembly are shown in figure 3B. Provision is made for mounting and sealing at both ends of the unit. These seals are typically designed for pressure differentials on the order of several psi -- much higher than needed for the present application.

In industrial applications, filter elements of this type are usually installed in close-fitting steel housings which attach to a cast header having pipe threads for fluid connection. This construction cannot be adopted without modification for the filter/separator application for reasons of weight and materials compatibility. Also, a relatively greater volume is needed on the outside of the element. This will allow the system liquid reservoir to be integral with the filter/separator. Introduction of the mixed phase stream to the element interior should be through a circular distributor to direct the flow gently against the inside of the element; and, of course, a gas take-off tube is needed.

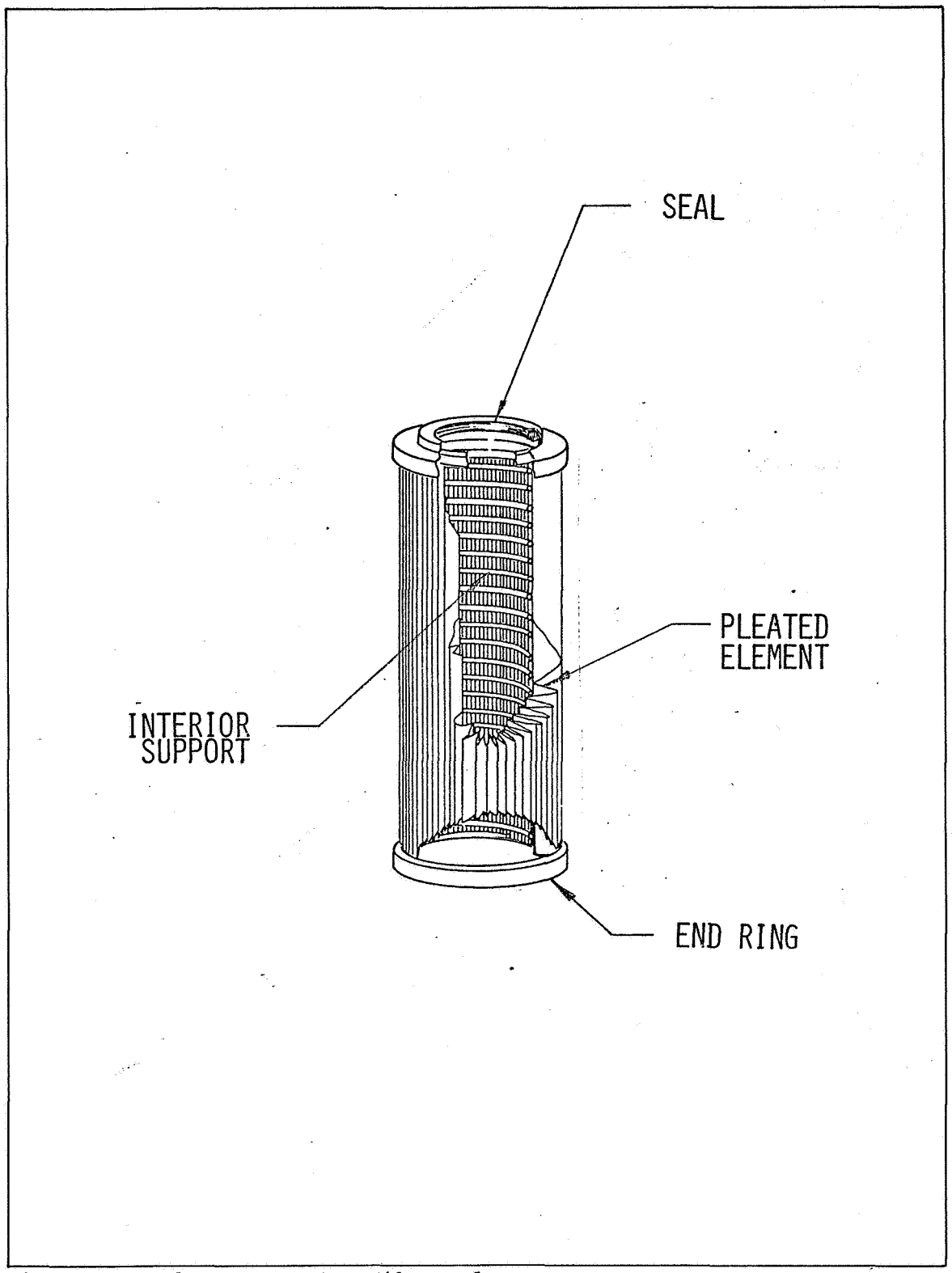


*Figure 3A. Phase Separator Filter Element*

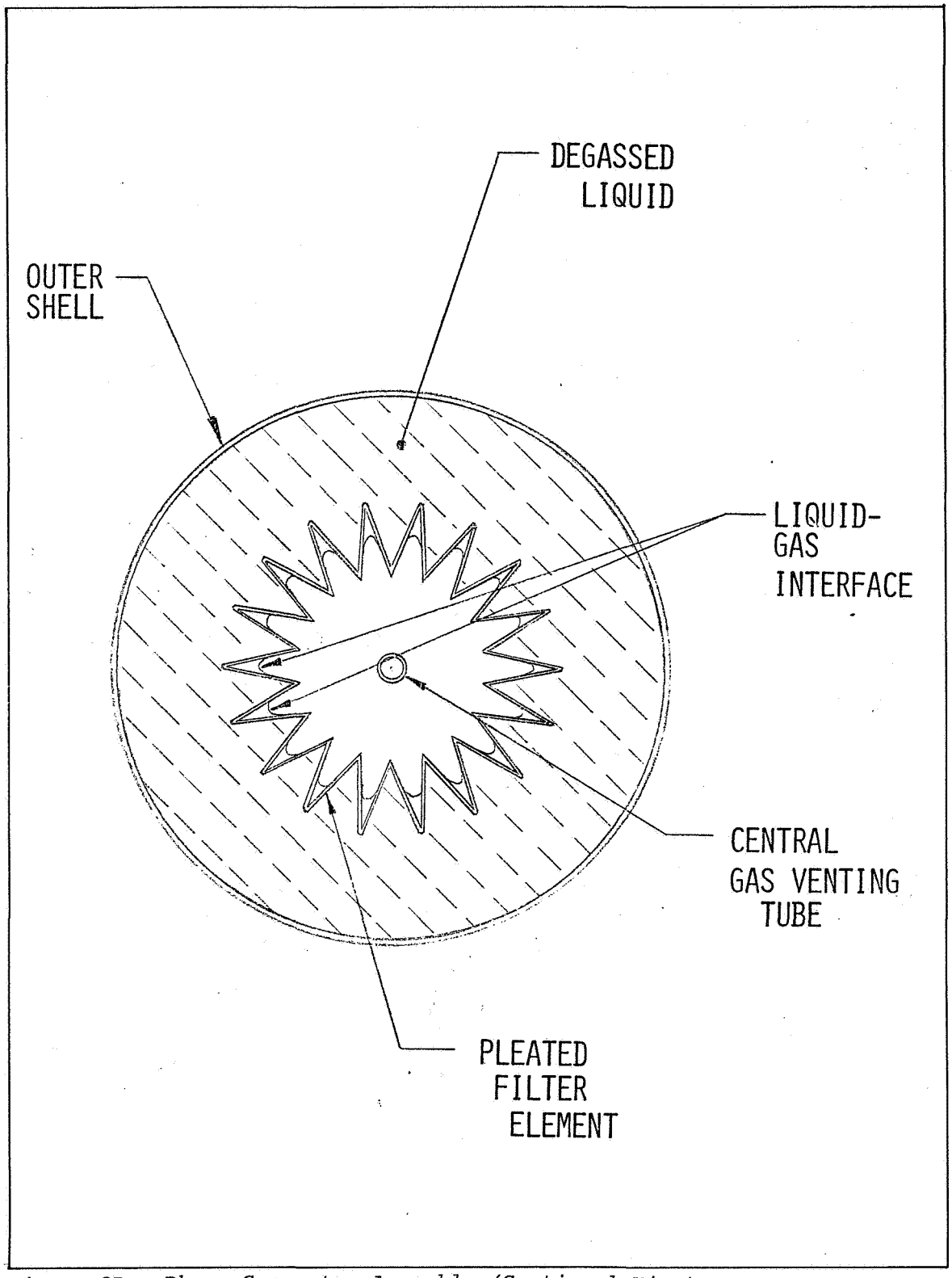


*Figure 3B. Phase Separator Assembly (Sectional View)*

All these requirements are best met by designing a special housing for the unit. This is facilitated by the simple geometry of the element. For instance, for a typical filter element two inches in diameter by seven inches long (Torite 8114, Torite Filter Corp., San Fernando, California 91340), the housing outside diameter would be about five inches to provide the desired one liter liquid volume. (About 150 cc of degassed liquid would be contained within the filter element pleats per se.

Fluid flow in the system is best understood by referring again to the flow schematic in figure 2. Pressure in the system is basically fixed by the requirement that evolved gases be vented to the atmosphere. Therefore, the high pressure side of the system is very slightly above atmospheric pressure. Liquid flow through the filter element is induced by the pump. Because pressure drop across the element is low, only a very slight vacuum will be induced at the pump inlet, minimizing any danger of cavitation. It may be desirable, in order to run the pump in a stable range of its operating characteristics, to run it at higher than minimal speed, and to use a throttling valve, as shown in figure 2, to reduce the pressure down to system requirements.

An important design consideration is the behavior of the liquid in the system under the influence of inertial forces at launch. As mentioned earlier, the best approach will probably be to completely fill the system with liquid initially, thus rendering it insensitive to inertial forces. In orbit, a few hundred cc's of liquid will then be drawn from the system to establish a gas space in the separator. This liquid will be slowly diverted to a storage sac from the three-way valve at the pump outlet. It is replaced by air drawn into the separator through the vent tube, thus establishing the gas space in the center of the assembly and the liquid/gas interface within the membrane folds.

The gases evolved at the cell electrodes will generally be a stoichiometric mixture of hydrogen and oxygen. Any possible hazard resulting from this can be handled in one of two ways. In our discussion to this point, we have shown the simple approach of limiting the quantity and pressure of gases present, and simply venting them through protective screen assembly or metallic frit. An

alternative approach is to employ two filter/separator units; one for the hydrogen and one for the oxygen. These separators would of course work in the same way as the one described. The effluents from the two units would join in a common line to the pump. There would, of course, be a slight weight penalty for using two units instead of one.

## 4.5 Pump Requirements

For effective flushing of gases from the electrode chambers, the system pump should deliver at least 5 ml per second per chamber. This is a total of 0.6 liters per minute, or approximately 9 gallons per hour. At this flow rate, the pressure drop across the electrode chambers has been measured at 20 inches of water column.

The total length of tubing (of assumed I.D. = 0.22 inch) in the rinse circuit will be about four feet maximum. Assuming about ten sharp elbows adding to the flow resistance, calculated total pressure drop across the tubing and fittings is 6.7 inches $H_2O$. Even in a 3 micron pore size, a commercial pleated filter element of suitable size incurs a pressure drop of only 6.5 inches $H_2O$ at the required flow rate. The total system pressure drop, then, is 20 + 6.7 + 6.5 = 34 inch $H_2O$, or approximately 1.2 psi. The system requirement on the pump is therefore 9 gallons per hour at 1.2 psi.

Given the low output pressure and the flow, several available laboratory-size pumps can meet the requirements. An additional requirement, however, is relatively smooth flow. Pulsatile flow is undesirable because bubble flow and electrical resistance in the electrode rinse circuit may be irregular, and because it may result in membrane movement. The latter effect could seriously disturb the separation process and the optical signal. For these reasons, pumps with pulsatile flow such as the piston, diaphragm, and peristaltic types were not considered. The search for a suitable pump was narrowed to centrifugal and gear types, and it was decided that a small centrifugal pump would be best. Performance curves for a pump of the selected type showed that there is ample margin in both pressure and delivery.

Centrifugal pumps have an inherently smooth output, and a favorable pressure-vs.-delivery curve. Their most serious drawback is that they are not reliably self-priming. This difficulty is overcome in the proposed system by proper location of the pump. The pump is in the output line from the phase separator, which delivers only gas-free liquid. This feature helps insure that there will be no vapor or air at the pump inlet which might cause a loss in pump priming.

As examples, two commercially available centrifugal pumps suitable for the application are the Cole-Parmer Model 7004-6 (Cole-Parmer, Chicago, Illinois 6064 ) and the Micropump Model 10-41-316 (Micropump Corp., Concord, California 94518). There are many others, as it is not an unusual or demanding pump application.

Measurement of pressure at the pump inlet is of interest because it can indicate filter/separator clogging as well as possible pump cavitation. For this reason, a pressure gage is indicated at that point in the flow schematic of figure 2.

### 4.6 Operation of the Rinse Flow Loop

Referring again to the rinse loop as shown schematically in figure 2, the centrifugal pump circulates electrode rinse liquid from the phase separator to the electrode chambers, and back to the phase separator. As set up on the ground prior to flight, the phase separator would be completely filled (i.e., contain no gas space). Valves A, B, and C would be closed until the system is ready for use. At that time, valves B and C are opened, and with valve D appropriately positioned, the pump is started. An expandable take-up sac attached to the side arm of valve D is filled with liquid from the phase separator to bring the meniscus in the separator to a position lying within the fluting. For normal operation of the system, valve D is now returned to its normal position, and valves A, B, and C are open.

## 5.0 PHASE MIXING

The phase materials and sample are injected into the cell by means of a hypodermic syringe. A "standpipe" at the exit side of the sample space, at least equal in capacity to the syringe, serves as a take-up for liquid volume in

excess of the sample chamber volume. The I.D. of the take-up tube is small enough (e.g., 1 cm) to contain the liquid safely by capillary action in microgravity. The syringe may initially be filled manually from a vessel which contains the two-phase material and has previously been shaken by hand. The sample cell suspension may then be taken up into the syringe from another container. Alternatively, the mixture of phase materials and sample could be pre-stored onboard in the hypodermic syringe. Our experiments (section 6.4 below and figure 4) show that the phase material is mixed very effectively by being alternately injected via the cell into the take-up tube, and drawn back into the hypodermic syringe. Three or four cycles suffice. As we point out later, this mixing action can be supplemented by the use of a small Teflon-coated iron ball in the syringe, the ball being moved back and forth in the syringe with an external magnet.

## 6.0 CELL DESIGN AND PERFORMANCE

### 6.1 Mechanical Design

A cell was fabricated as shown in figure 4. Experiments with the cell helped to verify general design concepts and permitted testing for electrode rinse behavior, optical performance and phase mixing.

The design shown may serve as the basis for a first experimental flight unit. Compared with final design requirements, it is simplified in that no provision is made for lateral displacement of the phases relative to each other, or for phase collection after the phases are electrically separated. The design nevertheless allows valuable information to be obtained on dynamics of the separation process under various conditions and with various phase compositions.

The cell body is a three-membered assembly of acrylic polymer. The middle member defines the sample chamber in which separation takes place. An inlet and o utlet are provided in this member for introduction of phase material and sample, and for mixing in the manner described. The upper and lower members contain the electrode chambers, each of which is ported for flow-through of electrode rinse medium. The electrode in each chamber is a three-wire platinum

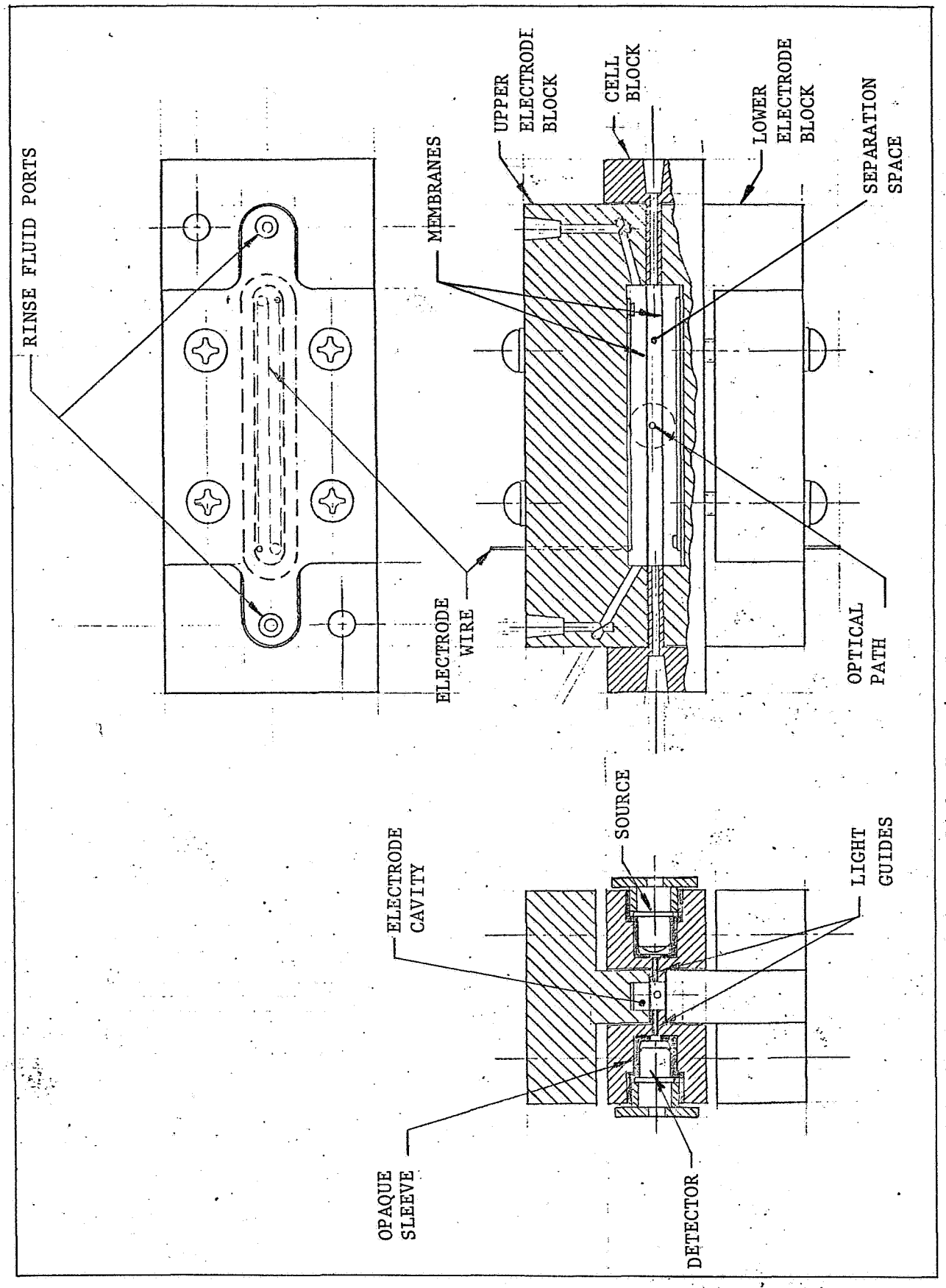


*Figure 4. CCD Cell for Preliminary Flight Experiment*

grid partially embedded in epoxy on the rear wall of the chamber and oriented along the chamber length. The membranes are cemented to the rim of each electrode chamber, or merely clamped between this rim and the shoulder that encircles the sample chamber. An improvement, if necessary at a later time, could be the provision of O-ring seals between the mating surfaces that join the inner and outer main members of the cell.

The radiation source and detector, flanking the separation space, are mounted in the side walls of the middle member.

## 6.2 Optical Design

The optical system is designed to monitor the clearance of the initially turbid two-polymer emulsion confined in the phase separation chamber. The principal optical components are an infrared source (Monsanto ME 7124) and a compatible phototransistor (Monsanto MT2) serving as a detector. A copy of the manufacturer's specifications for each of these is attached to this report. The source peaks at 940 nm, radiating in a narrow cone with a half-angle of six degrees. The detector response peaks at 830 nm, with 80% of peak response percent at 940 nm. Its angular response lies mainly within a cone of a twelve degrees half-angle.

Infrared radiation in the neighborhood of 940 nm is acceptable for this task. It is chosen because of the availability of the cited high energy, convenient, solid state source and compatible detector. Tests show that a 10% W/W polyethylene glycol 6000 has 74% transmittance at this wavelength for the 0.5 cm path of the CCD cell; the dextran T500 a transmission of 92% at this same concentration. Additionally, most of the emulsion micelles involved in light scattering during separation of the phases have a much larger diameter than the wavelength of either visible light or the near-infrared radiation used. Therefore, scattering is relatively independent of wavelength in this general wavelength range.

The optical arrangement is that of a turbidimeter, in the strict sense of an instrument that measures scattering by loss of light reaching a detector aligned with a direct beam from the source. Accordingly, separation of the phases,

resulting in a clearer medium, is accompanied by a signal increasing asymptotically toward a maximum.

The source and detector are each mounted within an opaque plastic thimble and held in place by means of a spacer member and backing plate (see figure 4). The thimbles are provided with 0.040" diameter apertures aligned with the optical axes of the source and detector. This defines an optical path passing across the width of the phase separation chamber.*

Tests with light directed onto the cell from various angles, and with room lights turned on and off, established that the thimbles isolate the source/detector system quite effectively from stray light. In the finalized assembly, it may be desirable also to pot the source and detector electrical leads within the mounting ferrules with an opaque embedding material such as silicone rubber.

In place of the Millipore filter material used to segregate the electrode chambers from the separation chamber during the flow tests, Mylar septa were used during the optical testing. This was done to avoid mass transfer of liquid across the membranes which might affect the measurements.

### 6.3 Electronics

Typical response for the MT2 phototransistor detector is roughly 600 μA per $mW/cm^2$ of irradiation on the detector face. The detector current is coupled to the amplifier shown in the attached schematic (figure 5). The output of the amplifier in volts per ampere input is 47,000, equal numerically to the amplifier feedback resistor value.

The amplifier output is fed to a chart recorder via an attenuator potentiometer. The amplifier output was zeroed with the source and room lights turned off. Monitoring the unattenuated amplifier output with the source turned on and the chamber filled with water gave a 3.5 V signal. With the source off and room

*In the device as built, the beam passes halfway between the membranes. It may be preferable, in later modifications, to pass the beam through the middle of the lower (e.g., PEG) phase.

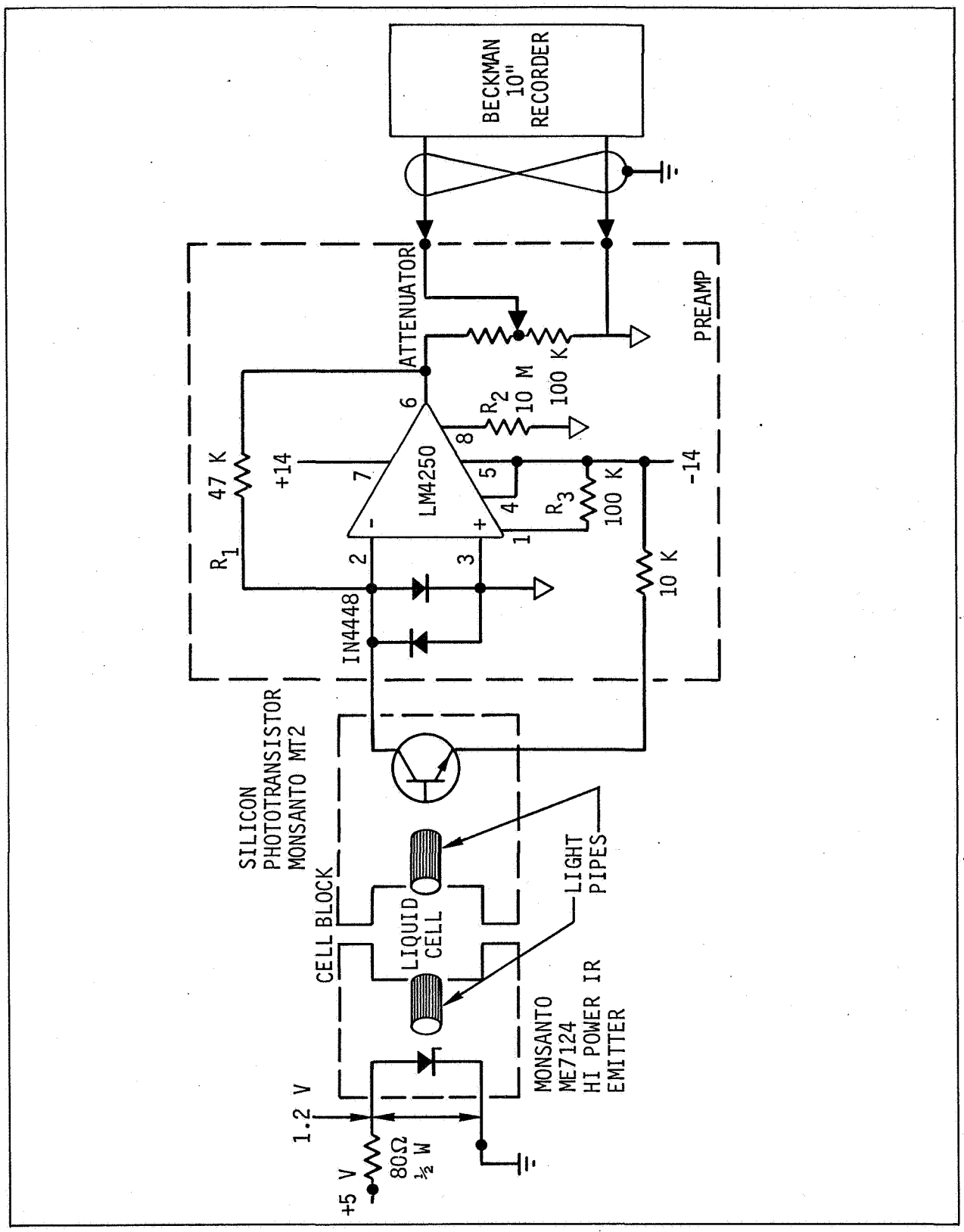


*Figure 5. Photometer Electronics*

lights on, the signal was about ten millivolts. The noise level, within the passband of the amplifier-recorder system, is too low to be detectable in the recording (using a Beckman 10" recorder). Seen on an oscilloscope of nominal 20 Mhz cutoff, the amplifier output noise was about 8 mv, peak to peak.

## 6.4 Operational Tests

A recording of phase separation (two successive runs) is shown in figure 6, using the polymer phases indicated above. The recorder was adjusted to full scale with a two-polymer mix that had been allowed to separate for several hours, Slow equilibration may have been due to alignment of the beam with the phase interface, where "tailing" of the separation may be most persistent.

The chamber receives the experimental emulsion by injection at one end of the cell with a syringe and flow of the excess into a standpipe at the other end. The syringe contains approximately 3 ml of each polymer solution. The mixture is pumped back and forth between the syringe and standpipe. A series of three or four strokes of the syringe piston is adequate to insure complete mixing of the two phases.

During the separation, and most conspicuously in an intermediate stage, globular masses of the separate phases moving across the beam result in a rather noisy optical signal.

The rapid oscillation of the signal seen in figure 6 at the beginning of each separation is an artifact of the mechanical mixing of the polymers. The low, well defined signal level immediately following indicates that the polymers are well mixed. Upon cessation of agitation, the emulsion immediately begins to clear. After about five minutes the signal shows large departures from the previously smooth trend, indicating the onset of the aforementioned globular migration.

# 7.0 SYSTEM PACKAGING CONCEPT

A packaging concept for the assembled space CCD experiment is shown in Figure 7. For transport and storage, the system is housed in an enclosure, the top

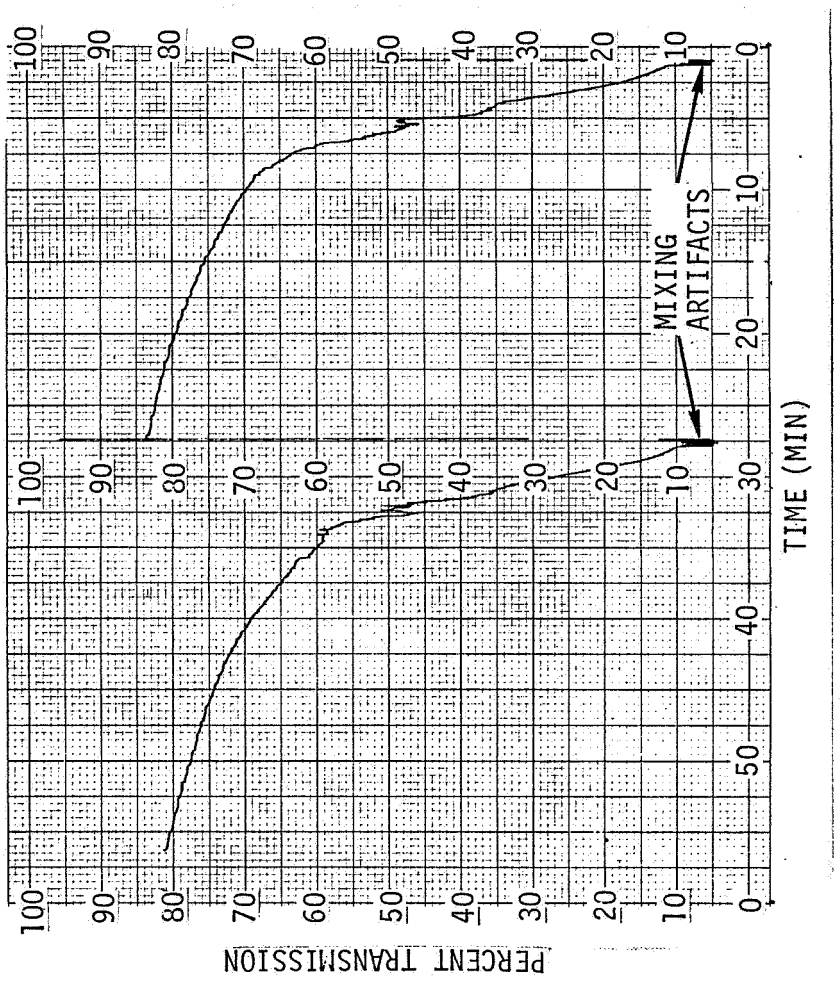


*Figure 6. Recording of Separation Process: Two Runs, Each Proceded by Syringe-Driven Mixing*

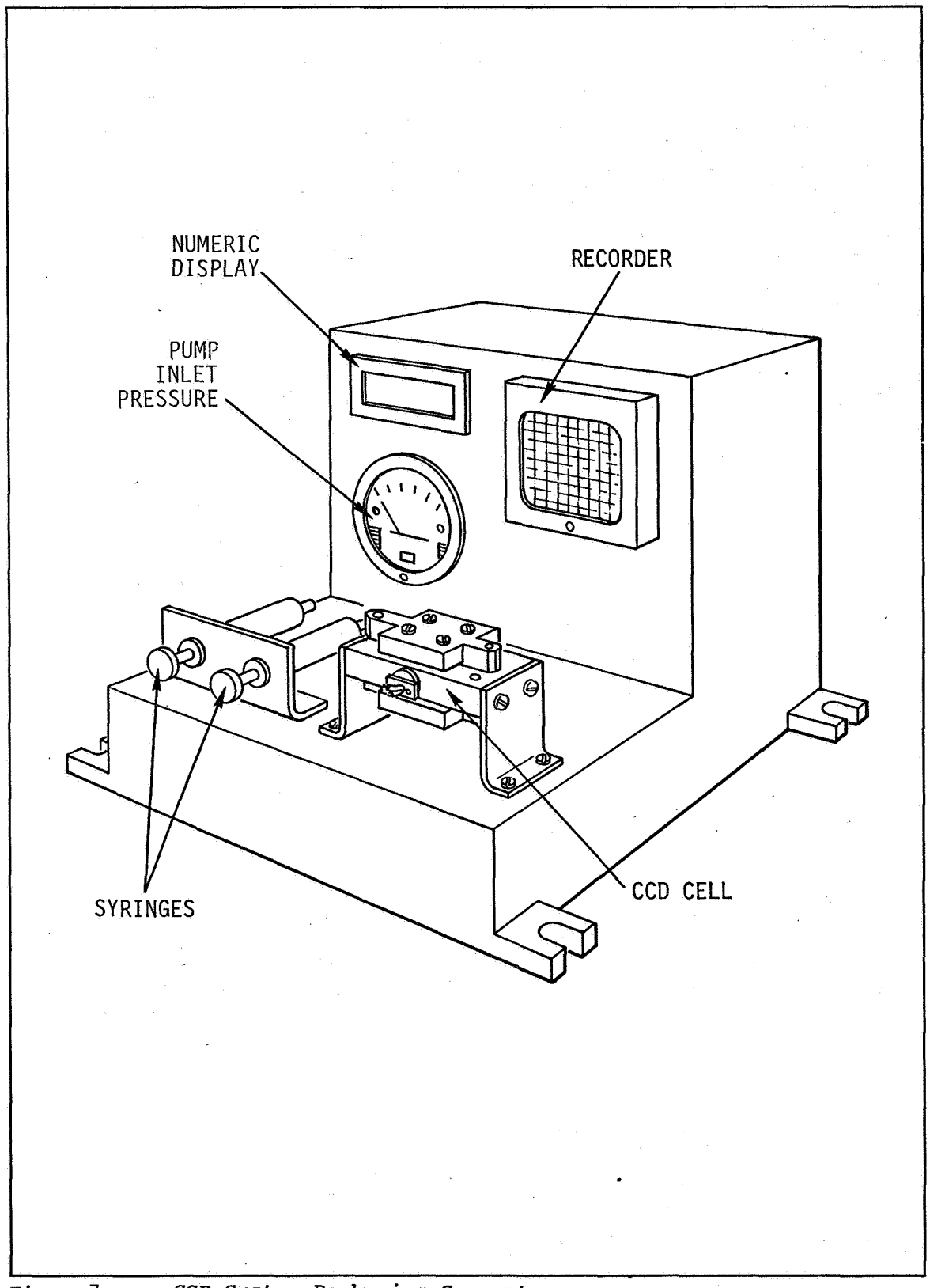


*Figure 7. CCD System Packaging Concept*

of which is removed for operation. The system comprises two main subassemblies. One includes the cell and all liquid handling components; the other the electronics, including power supplies for the optical source, cell field and amplifiers, the optical signal amplifier per se, the signal conditioner, and data interface provision. The two subassemblies may form a unitary structure as shown in figure 7, or comprise separate units connected by a cable. In either case, they are of a conformation and size designed to fit into a shuttle bay.

For ease of operation, the cell and liquid injection syringes are exposed. The pump and phase separator may lie behind the mounting panel, but will be accessible to view and manipulation to allow checking and correction for leaks, verification of bubble clearance, etc. The pump will be mounted on a vibration-isolated plate. The clear plastic cell is elevated from the base plate for good visibility and illumination. The sample injection and mixing syringes, which require operator manipulation, are located next to the cell.

The monitoring and control panel includes a small analog recorder and a numeric display for indicating cell voltage, current, cell temperature (if desired) and optical signal level. A gage indicates pressure at the pump inlet. This monitors the state of the phase separator filter, showing abnormally small negative pressure if the filter breaks, and excessive negative pressure if the filter clogs.

The monitoring panel also includes controls (not shown) for selecting the function displayed on the numeric readout, adjusting cell voltage, and adjusting the zero and gain of the optical signal amplifier.

## 8.0 ADAPTABILITY TO AUTOMATION

The system as described in this report was adapted primarily for manual operation. We were asked, however, during the study to consider what might be involved in automation or semi-automation of the system, since astronaut time available during flight might be limited, and pre-training on the ground minimal.

It is useful to consider first, with reference to figure 2, a typical sequence of steps that might be involved in a purely manual system:

1. Turn on electronics for warm-up; energize source and detector.

2. Valves B and C are opened, valve D turned to "drain" position, and the pump turned on until the take-up sac is filled.

3. Valve D is turned to "run" position, valve A opened and the pump restarted to fill and operate the electrode rinse loop.

4. Valve E is turned to "drain" position, and water or clear buffer injected by syringe into cell to fill the sample space. Adjust recorder to read 100% or full scale. Following this, inject air to remove the water or buffer from the cell.

5. Attach syringe filled with phase mixture or phases plus sample. If necessary, purge cell with a small portion of the syringe contents to remove residual water. In this case, to preserve the volume ratio of the phases, it may be desirable to premix the syringe contents, just before purging, using a magnetic ball in the syringe and an external magnet. Turn valve E to "normal" position.

6. Turn on recorder, cycle the phase mixture several times from the syringe through the cell and back; apply voltage to electrodes, and allow separation and recording process to proceed for predetermined time. To remix for repeat recording, or to separate the same mixture at a different applied voltage, again cycle mixture via cell and take-up tube, apply voltage, and record.

7. To run further experiments using different phase mixture or phase/sample, readjust 100% with water in cell, substitute new mixture in cell, and proceed as in steps 5 and 6 above.

Evidently, a fairly extensive set of manipulations is involved. Automation could eliminate the need for an experienced operator, obviate human error, facilitate liquid handling steps that might be awkward in microgravity, and free the operator for other tasks.

A fully automated system would introduce at least the following features:

1. Vessels containing the liquid media (phase materials, sample suspensions, wash water) would be "pre-plumbed" into the system.
2. Actuators (electromechanical or pneumatic) would be provided for the valves and syringes.
3. A programmable controller would be provided for automatic sequencing, recording of results, and if desired, the monitoring and/or recording of "housekeeping" data.

Complete automation would obviously greatly increase the cost of the system. The concept would also depart radically from the earlier premise of a phased effort starting with relatively simple, low cost equipment. It is therefore of interest to consider whether partial automation could provide a useful compromise in cost vs. required operator involvement.

As a first step toward partial automation, all the fluid containers could be made integral with the plumbing per 1) above. This could eliminate manual liquid transfer or liquid handling operations external to the equipment. It could reduce the experiments to a sequence of button pressing, valve turning and syringe actuation. Whether the small gain made in this way is worthwhile is problematical, since the alternative of external liquid handling may require nothing more than the transfer and insertion of syringes.

Any further degree of automation would require mechanizing the actuation of syringe and valves. Having done this (at high cost in engineering and testing), it would appear reasonable to complete the automation by adding an electronic programmer/controller at moderate additional cost. The alternative, short of electronic control of such a system, would be manual triggering of the actuators and switches by the operator, but this would hardly justify the complication and cost of providing mechanized valves and syringes. In sum, there appears to be little choice between a purely manual and fully automated system.

## 9.0 CONCLUSIONS AND RECOMMENDATIONS

The recommended first flight unit employs a simplified single separation chamber adapted for optical monitoring of phase and sample separation dynamics. A circulating loop of electrolyte serves both to remove electrolysis products from the vicinity of the electrodes, and to remove Joule heat generated in the cell. Cooling may be passive, using only the thermal capacity of the rinse medium (1 liter or more in volume). A hydrophilic filter assembly, using a fluted filter element, acts as a phase separator for removing electrolytically generated gases from the loop.

Reversible electrodes, as a means for avoiding rinse loop and gas removal requirements, do not appear feasible. This follows from the unusually high current density in the CCD cell, and the serious problem of interference by electrolytically generated ions. Salt bridges are an unsatisfactory solution to the ion interference problem, since at the high current densities they are unavoidably associated with very large volume-heating effects.

An effective and simple optical system comprises a near-infrared, narrow-angle solid state emitter and a compatible narrow-angle phototransistor, both fitted into the body of the CCD cell. A simple amplifier conditions the signal for recording and data interfacing as required.

Phase mixing is readily accomplished by flushing the phase compositions back and forth through the cell three or four times, using a syringe for injection at one end of the cell, and a take-up tube at the other end. Supplementary mixing can be provided by a magnetic ball in the syringe, agitated by an external magnet.

Automation of the system is feasible, but only at a many-fold increase of cost that does not appear justified in a system designed for preliminary exploratory experiments.

The system is adaptable to packaging in a relatively compact carry-on unit, requiring only to be plugged into the on-board power lines.

A logical next stage in this program is the design, construction and ground-based testing of a prototype flight unit.

## 10.0 REFERENCES


1. Albertsson, Per-Åke, Partition of Cell Particles and Macromolecules, 2nd ed. (Wiley-Interscience, New York, 1971).

2. Neihof, R., Nature, 185, 526 (1960).

3. Neihof, R., J. Colloidal and Interface Sci., 30, 128 (1969).

4. Lingane, J.J., "Electroanalytical Chemistry," Interscience Publishers, Inc., New York, 1953, p. 281.

5. Lingane, J.J., ibid., p. 286.

6. See recent issues of Proceedings of Annual Power Sources Conference, and Intersociety Energy Conversion Engineering Conferences (annual).

7. Petrash, D.A. and E.W. Otto, "Controlling the Liquid-Vapor Interface During Weightlessness," Astronautics and Aeronautics, p. 26 et seq. March 1964.

8. Tegart, J.R. and D.A. Fester, "Space Storable Propellant Acquisition System," J. Spacecraft, 12, No. 9, 544 (1975).

9. Abdalla, K.L., et al, "Liquid Transfer Demonstrations on Board Apollo 14 During Transearth Coast," NASA Report TMX2410, Lewis Research Center, National Aeronautics and Space Administration, November, 1971.

10. Otto, W.E., "Static and Dynamic Behavior of the Liquid-Vapor Interface During Weightlessness," Chem. Eng. Prog. Symp., Ser 62, (61), 158-177 (1966).

11. Hastings, L.J. and R. Rutherford III, "Low Gravity Liquid-Vapor Interface Shape in Axisymmetric Containers and a Computer Solution," NASA, George C. Marshall Space Flight Center, Technical Memorandum X53790, October 7, 1968.

12. Brooks, D.E., "Concept Verification Studies," Contract NAS8-32353, in response to AO-76-02 (University of Oregon Health Sciences Center), September 1977.

13. Abdalla, K.L., et al, "Liquid Transfer Demonstration on Board Apollo 14 During Transearth Coast," NASA Report TMX-210, Nov. 1971, Lewis Research Center, NASA Administration, Cleveland, Ohio 44135.

## 11.0 APPENDIX 1: TABLE OF VALUES

The following summarizes assumed, derived and experimental values relating to design and operation of the model CCD cell and associated equipment as described in the present report.

a. CCD Cell Dimensions

| | |
|---|---|
| Separation chamber: | 5.0 x 0.5 x 0.25 cm |
| Electrode chambers: | 5.0 x 0.5 x 0.30 cm |
| Electrode to membrane distance: | 0.30 cm |

b. Operating Conditions

| | |
|---|---|
| Electrical conductivity, $K_e$, (separation chamber and electrode space): | $5 \times 10^{-2}$ ohm$^{-1}$cm$^{-1}$ |
| Thermal conductivity, $K_t$, in separation chamber: | $1.5 \times 10^{-3}$ g cal cm$^{-1}$deg C$^{-1}$ |
| Electric field gradient: | 10 V/cm |
| Cell current (neglecting membrane resistance): | 1.25A |
| Wattage, separation space: | 3.13 W |
| Watts, total, including electrode chambers: | 10.6 W |
| Hydrogen and oxygen gas volumes generated per 4 minute run (20°C): | 37.4 and 18.7 ml, respectively |

c. Rinse Loop

| | |
|---|---|
| Total volume: | approx. 1 liter, minimum |
| Allowed number of thermally cumulative runs: | 10 |
| Rinse loop starting temperature: | ambient |
| Rinse loop temperature rise, 10 runs, (assumed adiabatic case): | 6.1°C |
| Pressure drop across filter/phase separator: | 6.5 inch water head |
| Pressure drop, total, in connecting lines: | approx. 10 inch water head |
| Pressure drop across combined electrode chambers: | 20 inch water head |

d. Optical System

| | | |
|---|---|---|
| Source: | Monsanto ME 7124 IR solid state emitter | |
| | Peak wavelength: | 940 nm |
| | Output power: | 3.0 mW, typical |
| | Typical half-angle: | 6 degrees |
| Detector: | Monsanto silicon photo-transistor MT2 | |
| | Peak response at 830 nm; 80% of peak at 940 nm | |
| | Sensitivity ($S_{CEO}$) | 600 $\mu A/mW/cm^2$ |
| | Angular reponse: | cone half-angle approx. 12° |
| Amplifier Transfer Character-istic: | volts out per $\mu$ amp input: | 0.047 |

# Monsanto

# HIGH POWER INFRARED EMITTERS

# ME7121, ME7124

## PRODUCT DESCRIPTION

This family of high power liquid phase epitaxial IR Emitters is designed to accommodate all needs of the emitter detector relationship. Products range from a wide angle power spread for non-critical detector location to sharp-angle concentration of power for detectors located a significant distance from the emitter. The devices can be mounted with a plastic pop-in, furnished upon request.

## PACKAGE DIMENSIONS

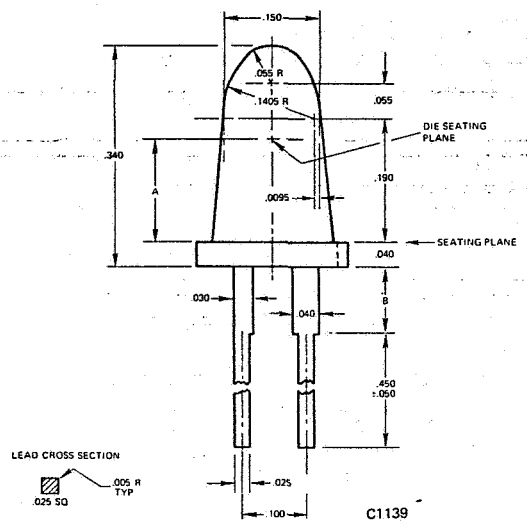


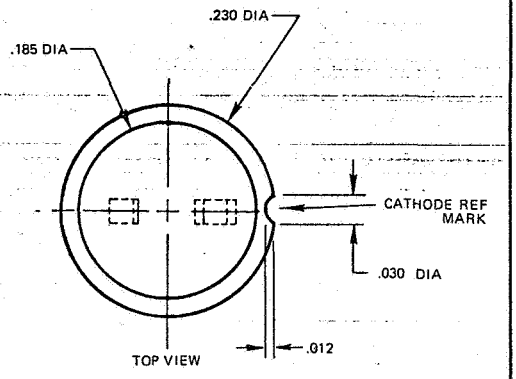


| DIM | A | B |
|---|---|---|
| ME7121 | .190 | .100 |
| ME7124 | .145 | .145 |

ALL DIMENSIONS IN INCHES
TOLERANCES = ±.010 UNLESS SPECIFIED

## ABSOLUTE MAXIMUM RATINGS

| | |
|---|---|
| Power dissipation @ 25°C ambient | 150 mW |
| Derate linearly from 50°C | 2.8 mW/°C |
| Storage & operating temperature | -55° to 100°C |
| Lead solder time @ 230°C (Note 3) | 5 sec |
| Continuous forward current | 100 mA |
| Reverse voltage | 3.0 V |
| Peak forward current (PW = 1.0 μsec, Duty Cycle = 0.3%) | 1.0 A |

## ELECTRO-OPTICAL CHARACTERISTICS

| | TYPICAL HALF ANGLE (DEGREES) | TYPICAL ON AXIS INTENSITY (MW/STR.) @ 50 mA | |
|---|---|---|---|
| ME7121 | 17° | 10.8 | into cone @ 1/2 power points @ $I_F$ = 50 mA ROP = 3 mW |
| ME7124 | 6° | 243.6 | |

| | MIN. | TYP. | MAX. | UNITS | TEST CONDITIONS |
|---|---|---|---|---|---|
| Total External Output Power (Note 2) | 1.0 | 3.0 | | mW | $I_F$ = 50 mA |
| Peak Emission Wavelength | | 940 | | nm | $I_F$ = 50 mA |
| Spectral Line Half Width | | 50 | | nm | $I_F$ = 50 mA |
| Forward Voltage | | 1.4 | 1.8 | V | $I_F$ = 50 mA |
| Light Turn On & Turn Off Time | | 500 | | nsec | 50 Ω Load |
| Reverse Current | | 10 | | μA | $V_R$ = 3.0 V |

## PANEL MOUNTING TECHNIQUES

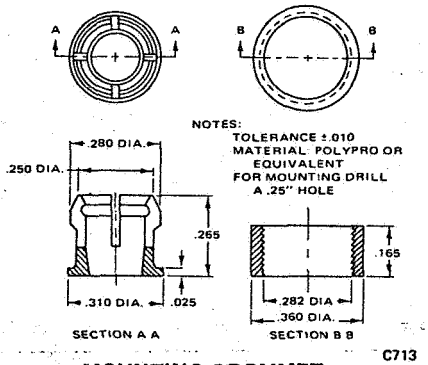


MOUNTING GROMMET

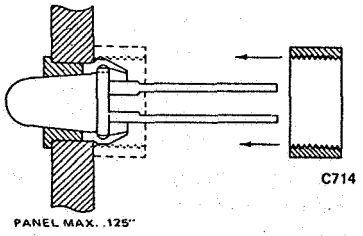


PANEL MOUNTING

## TYPICAL ELECTRO-OPTICAL CHARACTERISTIC CURVES

(25°C Free air temperature unless otherwise specified.)

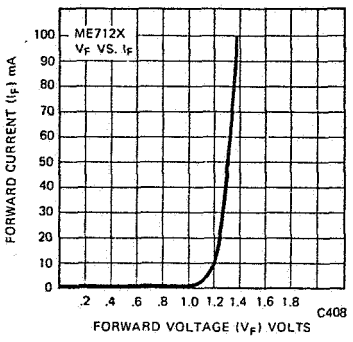


*Fig. 1. $I_F$ vs. $V_F$*

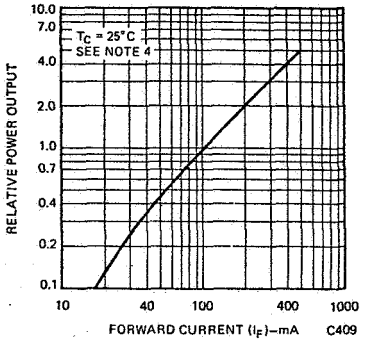


*Fig. 2. ROP vs. $I_F$ Peak*

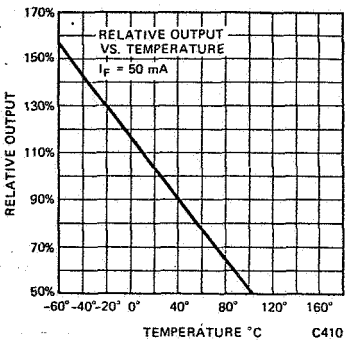


*Fig. 3. ROP vs. Temperature (Note 1)*

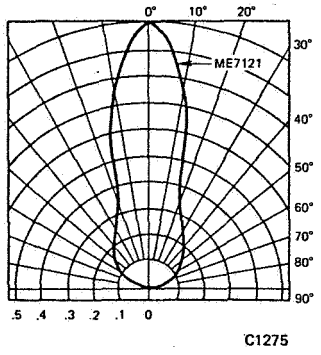


*Fig. 4. Spatial Distribution (ME7121)*

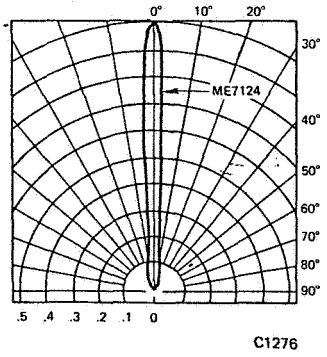


*Fig. 5. Spatial Distribution (ME7124)*

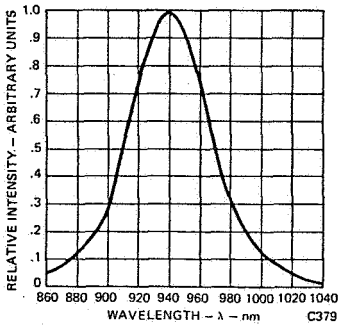


*Fig. 6. Spectral Distribution*

## NOTES

1. *The curves in figure 3 are normalized to the power output at 25°C to indicate the relative efficiency over the operating temperature range.*
2. *The total external radiated power output measurements are made with a Centralab 110C solar cell terminated into a 100Ω impedance.*
3. *The leads of the ME7121 and ME7124 were immersed in molten solder, heated to 230°C, to a point 1/16 inch from the body of the device, per MIL-S-750.*
4. *This parameter is measured using pulse techniques tw = 40 μsec duty cycle ⩽10%.*

# Monsanto

# SILICON PHOTOTRANSISTOR

**MT1**
**MT2**

## PRODUCT DESCRIPTION

The MT1 and MT2 silicon phototransistors are mounted on a standard TO46 header. The MT1 features a flat window mounted at the top of a protective metal can. The MT2 has a lens in the same position for optical gain of 4.

## PACKAGE DIMENSIONS

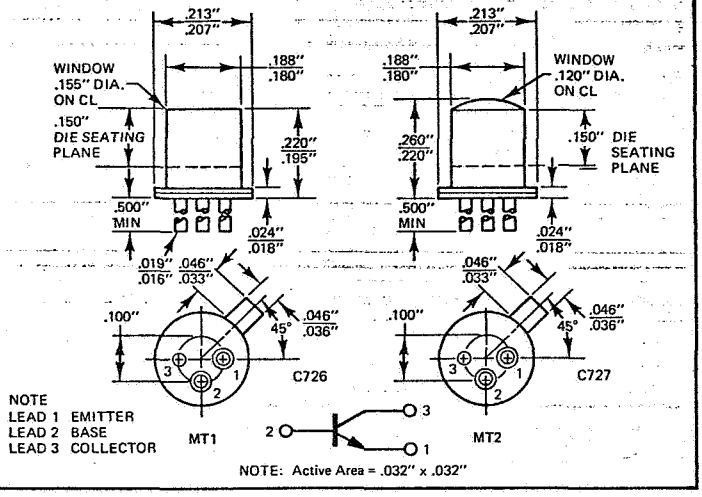


NOTE: Active Area = .032" x .032"

## FEATURES & APPLICATIONS

- Low leakage current - 1 nA
- Wide Spectral Response
- Responsive to GaAs - 1.40 mA/mW/cm$^2$
- Optional flat lens (MT1) or built-in optics (MT2)
- Standard Transistor (Hermetic Seal) package for easy handling and mounting

- Optical switching & encoding
- Intrusion Alarm
- Process Control
- Tape and Card Reader
- Level & Industrial Control
- Optical Character Recognition

## ABSOLUTE MAXIMUM RATINGS

Storage and Operating Temperature -55°C to 125°C
Maximum Lead Solder Time @ 260°C (See Note 1) - 7.0 sec

| | |
|---|---|
| Power Dissipation @ 25°C Ambient | 200 mW |
| Derate Linearly from 25°C | 2.0 mW/°C |
| Collector-Emitter Breakdown Voltage ($BV_{CEO}$) | 30 V |
| Emitter-Collector Breakdown Voltage ($BV_{ECO}$) | 7.0 V |
| Collector-Base Breakdown Voltage ($BV_{CBO}$) | 80 V |
| Collector Current ($I_C$) | 40 mA |

## ELECTRO-OPTICAL CHARACTERISTICS

(25° C Free Air Temperature Unless Otherwise Specified)

| CHARACTERISTICS & SYMBOLS | MIN. | TYP. | MAX. | UNITS | TEST CONDITIONS |
|---|---|---|---|---|---|
| Sensitivity MT1 (see note 3) ($S_{CEO}$) | 200 | 560 | | μA/mW/cm² | λ=0.9 microns, $V_{CE}$=5.0 V |
| Sensitivity MT2 (see note 3) ($S_{CEO}$) | 500 | 1400 | | μA/mW/cm² | λ=0.9 microns, $V_{CE}$=5.0 V |
| Sensitivity MT1 (see note 4) ($S_{CEO}$) | 80 | 260 | | μA/mW/cm² | 2875° K, $V_{CE}$=5.0 V |
| Sensitivity MT2 (see note 4) ($S_{CEO}$) | 200 | 650 | | μA/mW/cm² | 2875° K, $V_{CE}$=5.0 V |
| Sensitivity MT1 (see note 3) ($S_{CBO}$) | 1.4 | 2.5 | | μA/mW/cm² | λ=0.9 microns, $V_{CE}$=5.0 V |
| Sensitivity MT2 (see note 3) ($S_{CBO}$) | 3.5 | 6.2 | | μA/mW/cm² | λ=0.9 microns, $V_{CB}$=5.0 V |
| Sensitivity MT1 (see note 4) ($S_{CBO}$) | 0.6 | 1.0 | | μA/mW/cm² | 2875° K, $V_{CB}$=5.0 V |
| Sensitivity MT2 (see note 4) ($S_{CBO}$) | 1.5 | 2.5 | | μA/mW/cm² | 2875° K, $V_{CB}$=5.0 V |
| Collector-emitter saturation voltage ($V_{CE(sat)}$) | | 0.2 | 0.5 | V | $I_C$=2.0 mA, H=10mW/cm² |
| Light current rise time (see figure 8) ($t_r$) | | 2.0 | | μs | $V_{CC}$=5.0 V, $I_C$=2.0 mA, $R_L$=100Ω |
| Light current fall time (see figure 8) ($t_r$) | | 2.0 | | μs | $V_{CC}$=5.0 V, $I_C$=2.0 mA, $R_L$=100Ω |
| Delay time (see figure 8) ($t_d$) | | 1.2 | | μs | $V_{CC}$=5.0 V, $I_C$=2.0 mA, $R_L$=100Ω |
| Frequency response | | 300 | | kHz | $V_{CC}$=5.0 V, $I_C$=2.0 mA, $R_L$=100Ω |

## ELECTRICAL CHARACTERISTICS (25°C Free Air Temperature Unless Otherwise Specified)

| CHARACTERISTICS | SYMBOLS | MIN. | TYP. | MAX. | UNITS | TEST CONDITIONS |
|---|---|---|---|---|---|---|
| Collector dark current (see note 2) | $I_{CEO}$ | | 1 | 20 | nA | $V_{CE}$=5.0 V |
| Collector dark current (see note 2) | $I_{CBO}$ | | 0.15 | 10 | nA | $V_{CB}$=5.0 V |
| Collector base breakdown voltage (see note 2) | $BV_{CBO}$ | 80 | 140 | | V | $I_C$=100 μA |
| Collector emitter breakdown voltage (see note 2) | $BV_{CEO}$ | 30 | 65 | | V | $I_C$=100 μA |
| Emitter collector breakdown voltage (see note 2) | $BV_{ECO}$ | 7 | 12 | | V | $I_E$=100 μA |

## TYPICAL ELECTRO-OPTICAL CHARACTERISTIC CURVES

(25°C Free Air Temperature Unless Otherwise Specified)

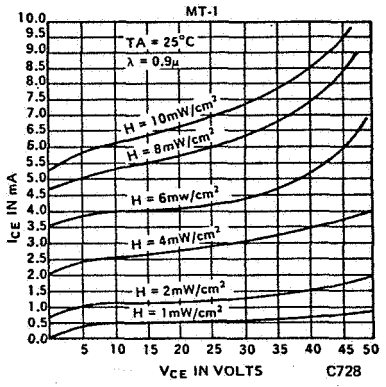


*Figure 1 Collector-Emitter Characteristics*

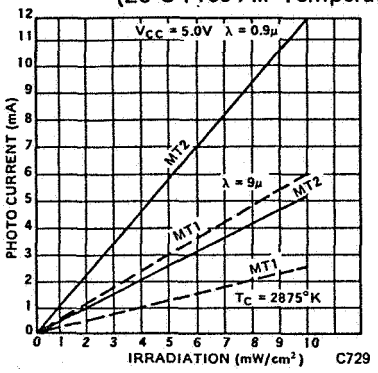


*Figure 2 Photo Current vs. Irradiation*

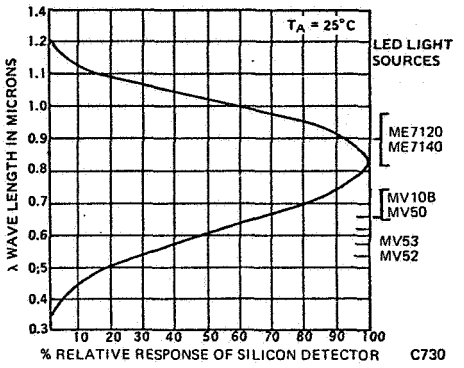


*Figure 3 Spectral Response*

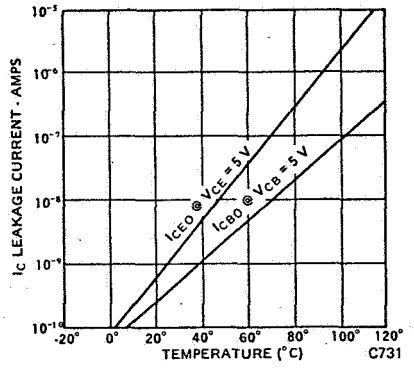


*Figure 4 Leakage Current vs. Temperature*

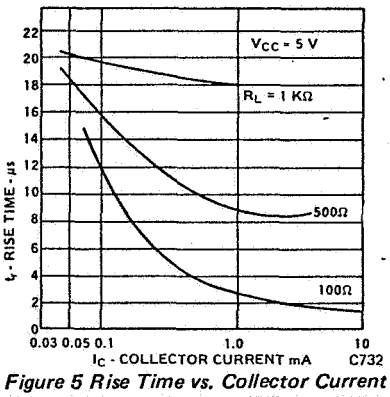


*Figure 5 Rise Time vs. Collector Current*

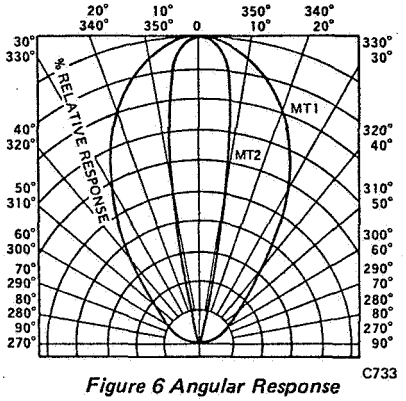


*Figure 6 Angular Response*

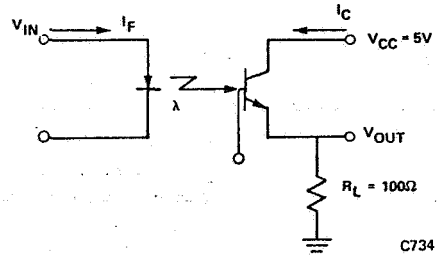


*Fig. 7 Circuit Used to Obtain Switching Time vs. Collector Current Plot*

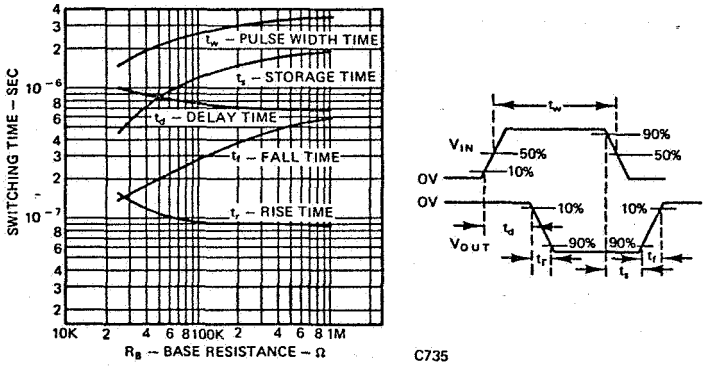


*Fig. 8 Switching Time vs. Base Resistance*

## NOTES

1. *The leads of the device were immersed in molten solder, heated to a temperature of 260°C, to a point 1/16-inch from the body of the device per MIL-S-750.*
2. *Measured under dark conditions H≤1.0μW/cm².*
3. *Measured with a GaAs light source at 0.9 microns with a radiation flux density of 3 mW/cm².*
4. *Measured with a tungsten filament lamp operated at a color temperature of 2875°K with a radiation flux density of 5 mW/cm².*